(4)

TECHNICAL REPORT BRL-TR-3013

BRL

TWO-DIMENSIONAL COMPUTER SIMULATIONS OF SEGMENTED PENETRATORS

DANIEL R. SCHEFFLER

JULY 1989

U.S. ARMY LABORATORY COMMAND

BALLISTIC RESEARCH LABORATORY
ABERDEEN PROVING GROUND, MARYLAND

DESTRUCTION NOTICE

Destroy this report when it is no longer needed. DO NOT return it to the originator.

Additional copies of this report may be obtained from the National Technical Information Service, U.S. Department of Commerce, Springfield, VA 22161.

The findings of this report are not to be construed as an official Department of the Army position, unless so designated by other authorized documents.

The use of trade names or manufacturers' names in this report does not constitute indorsement of any commercial product.

DISCLAIMER NOTICE

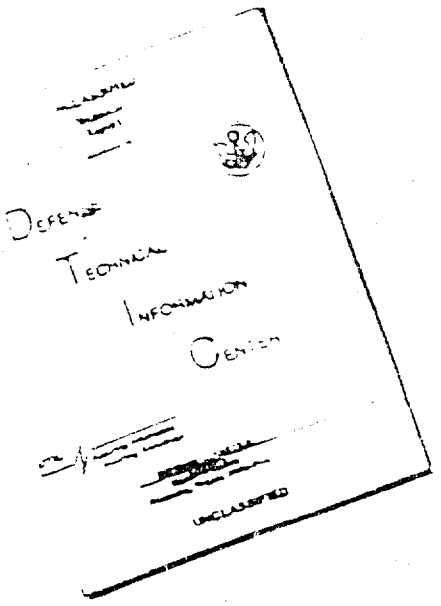

THIS DOCUMENT IS BEST QUALITY AVAILABLE. THE COPY FURNISHED TO DTIC CONTAINED A SIGNIFICANT NUMBER OF PAGES WHICH DO NOT REPRODUCE LEGIBLY.

UNCLASSIFIED

SECURITY CLASSIFICATION OF THIS PAGE

REPORT DOCUMENTATION PAGE

Form Approved OMB No. 0704-0188

1a. REPORT SECURITY CLASSIFICATION: UNCLASSIFIED	1b. RESTRICTIVE MARKINGS
2a. SECURITY CLASSIFICATION AUTHORITY	3. DISTRIBUTION/AVAILABILITY OF REPORT: APPROVED FOR PUBLIC RELEASE: DISTRIBUTION UNLIMITED.
2b. DECLASSIFICATION/DOWNGRADING SCHEDULE	
4. PERFORMING ORGANIZATION REPORT NUMBER(S): BRL-TR-3013	5. MONITORING ORGANIZATION REPORT NUMBER(S)
6a. NAME OF PERFORMING ORGANIZATION: Ballistic Research Laboratory; 6b. OFFICE SYMBOL (If applicable): SLCBR-TB	7a. NAME OF MONITORING ORGANIZATION
6c. ADDRESS (City, State, and ZIP Code): Aberdeen Proving Ground, MD 21005-5066	7b. ADDRESS (City, State, and ZIP Code)
8a. NAME OF FUNDING/SPONSORING ORGANIZATION; 8b. OFFICE SYMBOL (If applicable)	9. PROCUREMENT INSTRUMENT IDENTIFICATION NUMBER
8c. ADDRESS (City, State, and ZIP Code)	10. SOURCE OF FUNDING NUMBERS

PROGRAM ELEMENT NO.	PROJECT NO.	TASK NO.	WORK UNIT ACCESSION NO.
1L162618AH80			

11. TITLE (Include Security Classification): 2-D Computer Simulations of Segmented Penetrators

12. PERSONAL AUTHOR(S): Scheffler, Daniel R.

13a. TYPE OF REPORT	13b. TIME COVERED	14. DATE OF REPORT (Year, Month, Day)	15. PAGE COUNT
Final	FROM _____ TO _____		

16. SUPPLEMENTARY NOTATION

17. COSATI CODES			18. SUBJECT TERMS (Continue on reverse if necessary and identify by block number)	
FIELD	GROUP	SUB-GROUP		
19	04		Penetrator Efficiency	Computer/Numerical Simulation
			Segmented Penetrator	Kinetic Energy Penetrator
			HULL Hydrocode	Impact

19. ABSTRACT (Continue on reverse if necessary and identify by block number)

It has been shown that penetrator efficiency, i.e. the ratio of penetration to penetrator length (P/L), increases as the ratio of the penetrator length to diameter decreases (L/D). This suggests a long rod penetrator divided in several smaller length segments separated at a distance should improve performance when performance is measured in terms of total penetration. Numerical simulations are presented examining the performance of A. C.Charters 7 segment 18 gram kinetic energy penetrator at normal impact against a semi-infinite T4340 steel target. The two dimensional simulations compare the effects of the spacers used in Charters penetrator with a similar penetrator without spacers; compare the performance of equivalent mass and diameter and equivalent mass and length monolithic penetrators to that of their segmented counterpart at velocities of 3.4 and 4.0 km/s; examine the effects on performance of spacing-to-diameter ratio; and examine the use of penetration efficiency as a measure of the performance of segmented penetrators.

20. DISTRIBUTION/AVAILABILITY OF ABSTRACT	21. ABSTRACT SECURITY CLASSIFICATION
☒ UNCLASSIFIED/UNLIMITED ☐ SAME AS RPT. ☐ DTIC USERS	UNCLASSIFIED
22a. NAME OF RESPONSIBLE INDIVIDUAL	22b. TELEPHONE (Include Area Code) / 22c. OFFICE SYMBOL

DD Form 1473, JUN 86 *Previous editions are obsolete.*

SECURITY CLASSIFICATION OF THIS PAGE

UNCLASSIFIED

TABLE OF CONTENTS

Next page is blank.

LIST OF FIGURES

Next page is blank.

1. INTRODUCTION

It has been shown[1] that penetrator efficiency, i.e. the ratio of penetration to penetrator length (P/L), increases as the ratio of the penetrator length to diameter decreases (L/D). This suggests a long rod penetrator divided in several smaller length segments separated at a distance should improve performance when performance is measured in terms of total penetration. This has in fact been verified both analytically[2,3,4] and experimentally[5,6,7,8]. It is thought that if the separation distance between segments is optimum that each segment acts as an individual penetrator; thus the total penetration is the penetration of a single segment times the number of segments. These increases in performance generally require that the projectile be fired at greater than present ordnance velocities, i.e. 2 km/s, sparking interest in guns such as electro-magnetic guns[9] which can deliver projectiles into the hyper-velocity regime.

One researcher, A. Charters[1,5,7,8], has conducted a limited number of experiments of segmented and monolithic penetrators against both semi-infinite targets and spaced target arrays. The results obtained for normal impact into semi-infinite 4340 steel show segmented penetrators outperforming their equivalent mass and diameter monolithic penetrators by as much as 50 to 60 percent. Although it is believed that segmented penetrators improve performance, there is some skepticism about the results obtained in these tests. This paper documents a series a computer simulations using version 121 of the HULL finite-difference code examining the results obtained for Charters' 18 gram 7 segment penetrator. Figure 1 shows Charters' results obtained for this penetrator as well as those of an equivalent mass and diameter monolithic penetrator.

HULL[10,11] is an Eulerian wave propagation code that uses a second order accurate finite-difference scheme. The material advection scheme is first order. The code solves the partial differential equations of continuum mechanics ignoring heat conduction and viscosity terms. The Mie-Gruneisen equation of state is used to model solids and liquids. After vaporization occurs the Gamma Law equation is used to model the gas. Explosives can be modeled using the Jones-Wilkins-Lee equation of state. Material failure models include: maximum principal stress, maximum principal strain, and the Hancock-Mackenzie triaxial failure model[12]. When material failure occurs a numerically significant void, i.e. air, is introduced in the cell which permits relaxation of the tensile forces. Recompression is permitted.

Large-scale simulations are well suited for the study of segmented kinetic energy penetrators, increasing both our understanding of the penetration process and supplementing the limited ballistic test data. Furthermore computer studies permit the examination of segmented penetrators without the typical problems encountered in ballistic tests such as alignment of the individual segments, constraints of pre-extended projectile lengths, projectile yaw, structural integrity of the launch package, and synergistic effects of carrier tubes or carrier rods (spacers) on overall penetration.

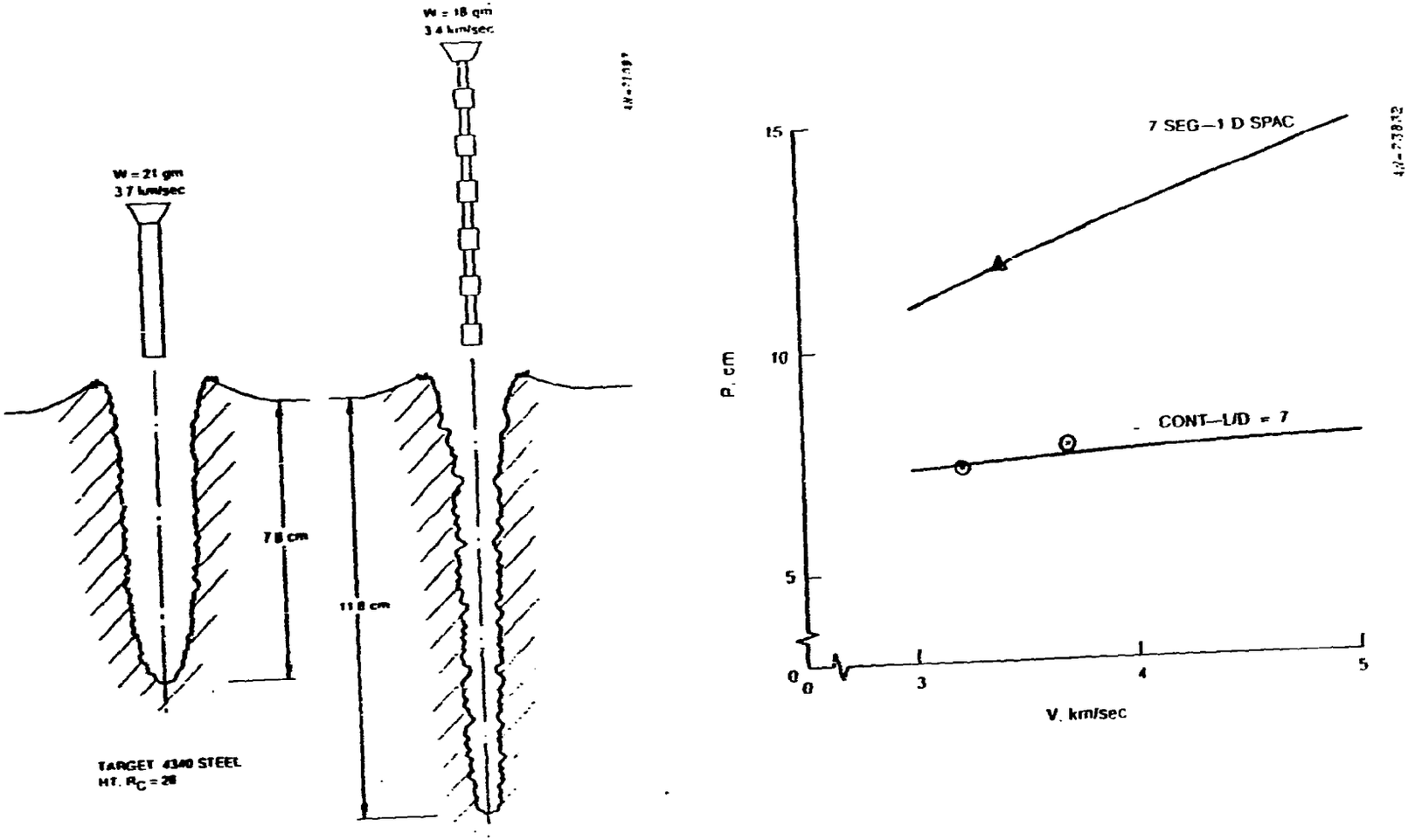

Figure 1. Charters' Segmented and Monolithic Rod Results (Ref. 7).

2. SIMULATION MATRIX

A series of two-dimensional simulations examining the performance of Charters' 18 gram 7 segment penetrator against a semi-infinite 4340 steel target have been conducted. A similar segmented penetrator without carrier rods has been modeled to characterize the effects of striking velocity (3, 3.4, and 4.0 km/s), spacing to diameter ratio, S/D, (1.4, 2, and 3); and the carrier rods on penetration performance. Penetrator performance is also compared to that of an equivalent mass and diameter and an equivalent mass and length monolithic penetrator for various striking velocities. Single segments were modeled to determine the maximum penetration possible at a given striking velocity. The complete computational matrix is given in Table 1.

The penetrator geometry used by Charters, Figure 2, was obtained by G. Silsby in a conversation with Charters[13,14] and later verified in a letter[15]. The S/D ratio was actually greater than unity, see Figure 1 and 2, and is approximately 1.38. The geometry of the penetrators used in the simulation are shown in Figure 3. The S/D ratio for the segmented penetrators was increased to 1.4 to allow for an integer number of cells between segments. The titanium connectors were not modeled because cell sizes needed to sufficiently resolve them would increase the problem size significantly. Also, due to their small mass and density, it is assumed that they caused no significant contribution to penetration.

In an effort to preserve material interfaces and minimize material diffusion typically encountered in Eulerian codes, a constant cell size was used in the axial direction. To keep problem size down a rezoner option was used. The rezoner causes the mesh to translate at the velocity defined by a Lagrangian tracer particle embedded in the front of a projectile. The segments consisted of 12 cells across the radius and 25 across the length, excluding spacers. Spacers had 4 cells across their radius. To keep track of the segments Lagrangian tracer particles were embedded in the front an rear of each segment and also in the front and rear of monolithic penetrators.

The hydrodynamic behavior of the metals were modeled using the Mie-Gruneisen equation of state. The coefficients for the equation data were obtained from the HULL Users Manual[11].

An incremental elastic-plastic formulation following the description given by Wilkins[16] is used to describe the strain response of the metals. An elastic-perfectly plastic model has been used for the 4340 steel with a 11.4 kb[17] yield strength. An elastic-strain-hardening-plastic model was used for the tungsten with a yield strength of 14.0 kb[18] and an ultimate strength of 19.3 kb[18]. A complete listing of the material properties and equation of state data are provided in the Appendix.

Table 1: SIMULATION MATRIX

Problem No.	Velocity (km/s)	N*	S/D	Mass (g)	Length (cm)	Length* (cm)	Penetration (cm)
10.1788	3.4	7	1.4	17.5594	3.8780**	8.5316	11.80
10.1988	3.4	7	1.4	16.1720	3.8780	8.5316	9.499
10.2088	3.4	1	0.0	16.1720	3.8780	3.8780	7.241
10.2188	3.4	7	2.0	16.1720	3.8780	10.5260	9.785
10.2288	3.4	7	3.0	16.1720	3.8780	13.8500	9.891
10.2388	3.4	1	0.0	2.3103	0.5540	0.5540	1.427
10.2488	3.0	7	1.4	16.1720	3.8780	8.5316	8.715
10.2588	4.0	7	1.4	16.1720	3.8780	8.5316	10.59
10.2788	3.4	1	0.0	16.1714	8.5316	8.5316	13.07
10.2388	4.0	1	0.0	16.1714	8.5316	8.5316	14.60
11.0188	3.0	1	0.0	2.3103	0.5540	0.5540	1.307
11.0288	4.0	1	0.0	2.3103	0.5540	0.5540	1.618
11.0388	4.0	1	0.0	16.1720	3.8780	3.8780	8.174
11.1088	6.0	1	0.0	16.1720	3.8780	3.8780	8.431

* Note: N=1 implies a monolithic rod.
Length implies overall length.
**Note: Length does not include contribution of spacers.

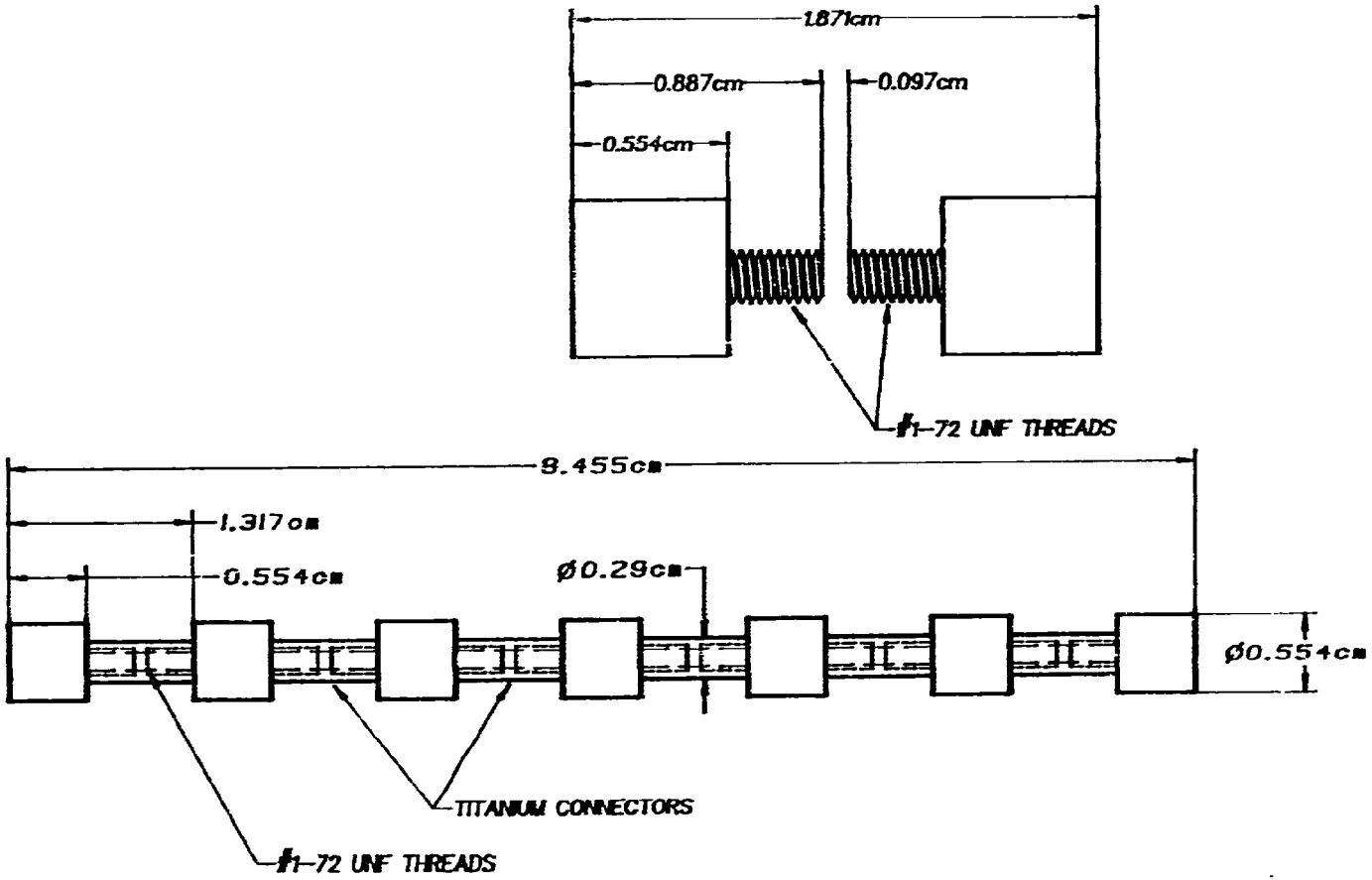

Figure 2. Charters' Segmeated Penetrator Geometry.

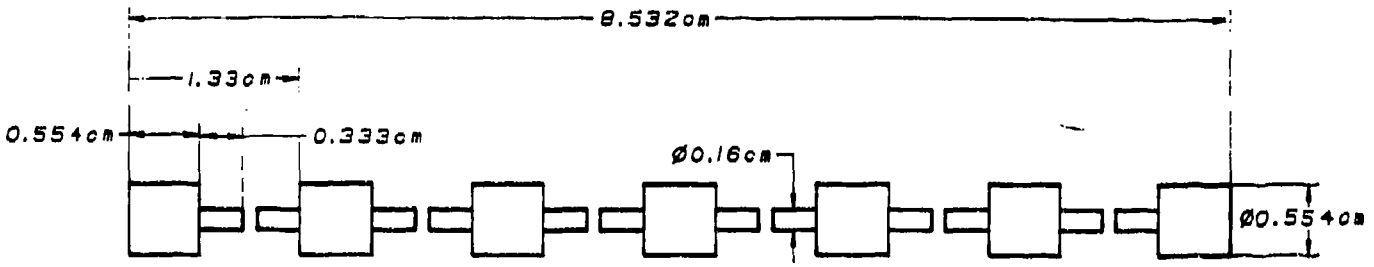

CHARTERS ORIGINAL 7 SEGMENT PENETRATOR

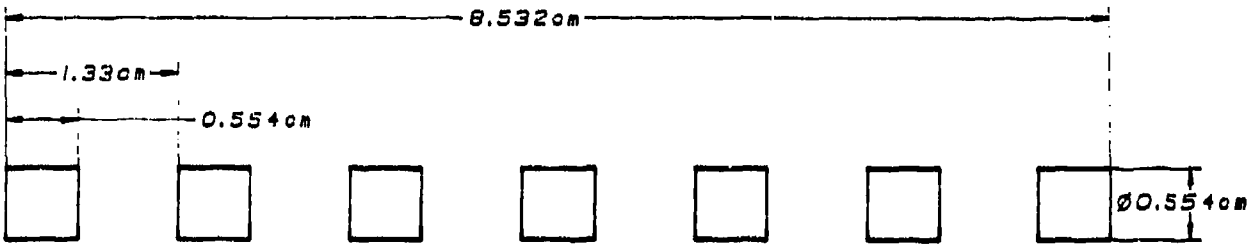

CHARTERS SEGMENTED PENETRATOR WITHOUT SPACERS

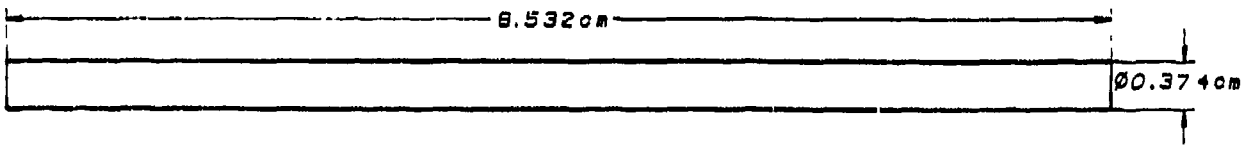

EQUIVALENT MASS EQUIVALENT LENGTH MONOLITHIC PENETRATOR

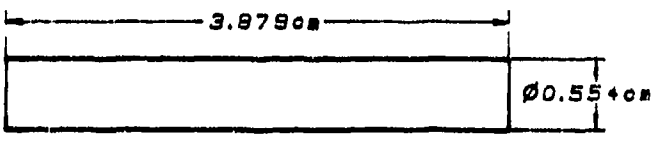

EQUIVALENT MASS EQUIVALENT DIAMETER MONOLITHIC PENETRATOR

Figure 3. Penetrator Geometries Used in Simulation.

3. RESULTS AND DISCUSSION

3.1 Effects of Carrier Rods

The simulation predicts the segmented penetrator with carrier rods will penetrate 11.8 cm of semi-infinite 4340 steel. This is in excellent agreement with Charters' experiment in which a penetration of 11.8 cm was obtained. The mass of the penetrator in the simulation was 17.56 grams. The penetrator used in experiment had a mass of 18.35 grams including the stablizing flare and 17.93 excluding the flare. The segmented penetrator without carrier rods had a mass of 16.17 grams or 7.9 percent less mass than the segmented penetrator with carrier rods used in the simulation. Since the mass of the carrier rods is small when compared with that of the penetrator, it seems reasonable that their contribution to penetration is also small. This, however, was not the case. The penetration for the penetrator without carrier rods was 9.5 cm or 19.5 percent less than that of the penetrator with carrier rods.

3.2 Monolithic vs. Segmented Penetrators

The performance of the segmented penetrator without carrier rods was compared to the performance of two equivalent mass monolithic penetrators. One had the same mass and diameter as the segmented penetrator and the other had the same mass and overall length. No comparisons between experiments exist for the segmented penetrator without carrier rods or the equivalent mass and length monolithic penetrator. However, good agreement exists between results obtained in experiment and simulation for the equivalent mass and diameter monolithic penetrator and the segmented penetrator with carrier rods, see Figure 4. The mass of the monolithic penetrator used in the experiment was approximately 19 grams or about 17 percent greater the that used in the simulation. Based on the good agreement obtained between experiment and simulation, it is estimated that the predicted results for which no experimental data exist, are within 10 percent of actual values.

Figure 4 shows a predicted increase in penetration of 31 percent for the segmented penetrator and 80 percent for equivalent mass and length monolithic penetrator over the equivalent mass and diameter monolithic penetrator at 3.4 km/s. The performance of the equivalent mass and length penetrator shows a predicted 11 percent increase in penetration over the segmented penetrator with carrier rods even though the segmented penetrator has 8.6 percent more mass.

3.3 Segment Spacing

The penetrator efficiency, penetration per unit penetrator length, increases as the length-to-diameter ratio, L/D ratio, decreases. This means that a penetrator with a L/D ratio of 7 cut into seven segment with a L/D ratio of 1 and separated at a distance should improve penetrator performance, when measured in terms of total penetration. In theory, if the separation distance is at optimum the maximum penetration for a particular segmented penetrator is the penetration obtained by a single segment times the total number of segments. To determine the optimum spacing the segment penetrator without carrier rods was studied for spacing-to-diameter ratios, S/D ratios, of 0, 1.4, 2.0 and 3.0 at 3.4 km/s. Results were compared with the maximum penetration obtainable based on a single segment calculations. Results are given in Figure 5.

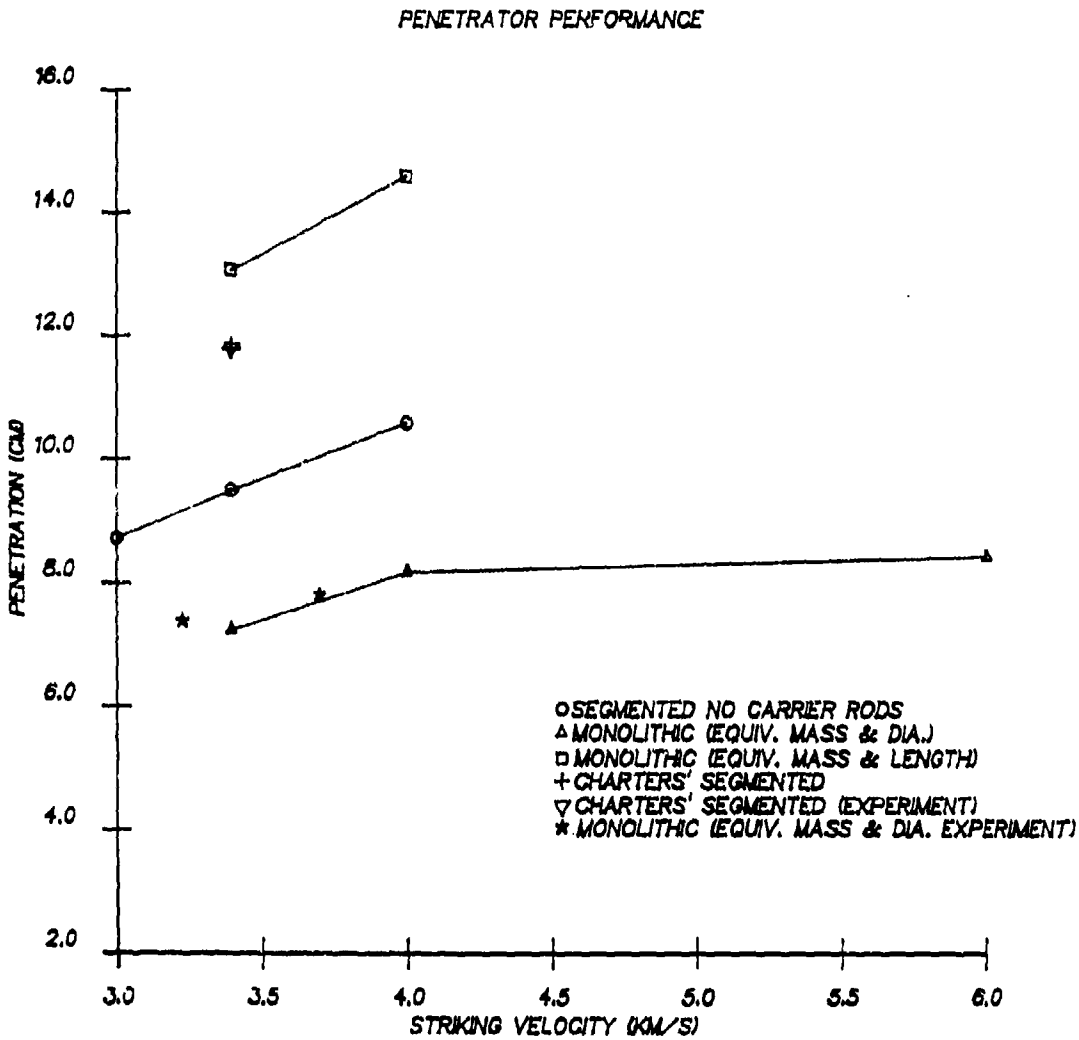

Figure 4. Experimental and Predicted Results.

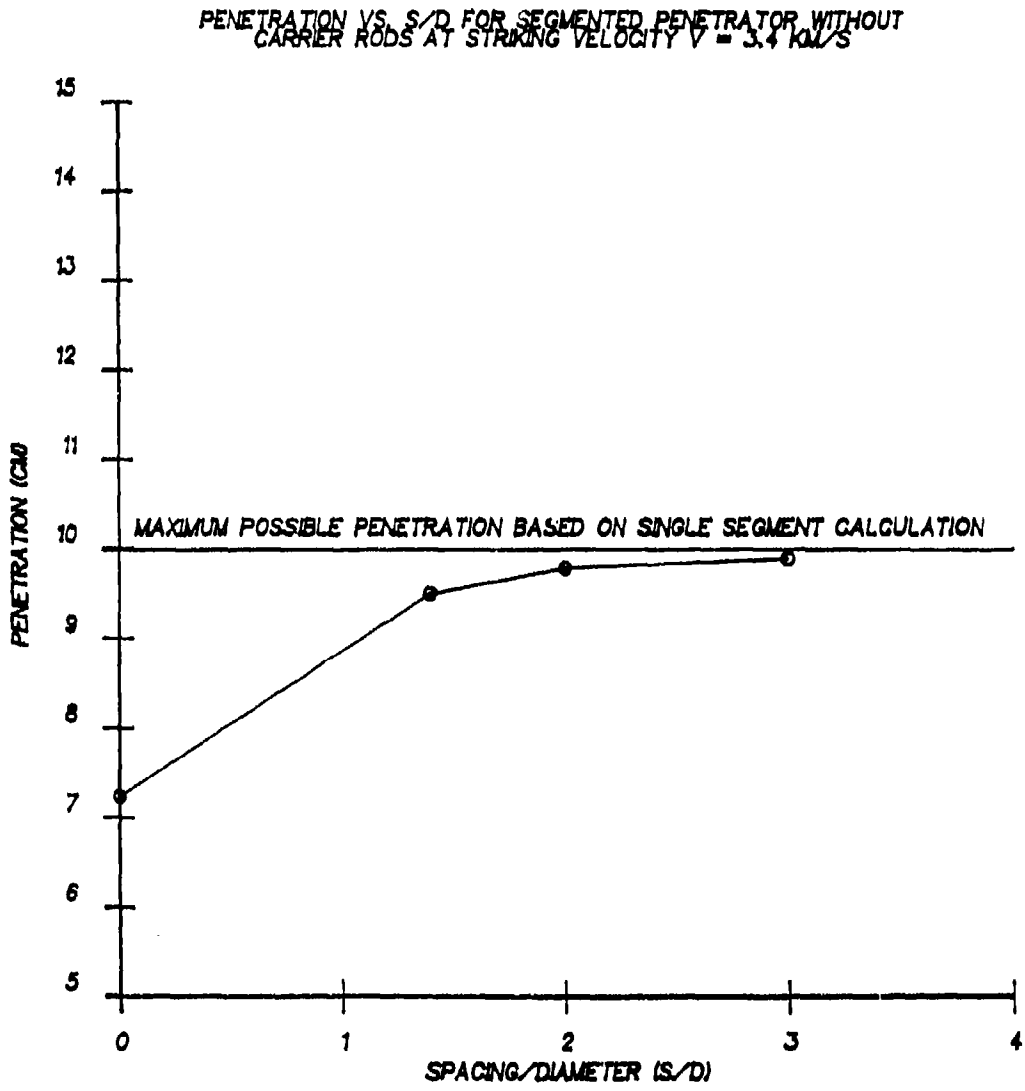

Figure 5. Predicted Penetration as a Function of Segment Spacing.

Figure 5 shows that the maximum possible penetration, given an infinite spacing, is 10.0 cm. Large increases in penetration are seen as the S/D ratio is increased from 0 to 1.4. The increase in penetration going from a S/D ratio of 2 to 3 is about 1 percent. At an S/D ratio of 3 the predicted penetration is within 1 percent of the predicted maximum. When the maximum predicted penetration is compared with that of the segmented penetrator with carrier rods it is still 15 percent less.

The segmented penetrator without carrier rods and S/D ratio of 1.4 was also studied at velocities of 3.0, 3.4 and 4.0 km/s. Results were compared with the maximum possible penetration based on single segment calculations, see Figure 6. The difference in predicted penetration and maximum predicted penetration at 3.0, 3.4 and 4.0 km/s is 5.0, 5.2 and 7.0 percent, respectively. This trend seems to indicate that a larger S/D ratio is needed at higher velocities.

3.4 Use of P/L as Penetration Measure

The use of penetration efficiency, penetration per unit length penetrator, is frequently used as a measure of penetrator performance. This is generally a good measure when used in the discussion of monolithic penetrators. However it can be ambiguous when discussing segmented penetrators. Typically in the discussion of segmented penetrators the length used in P/L is that of the equivalent mass and diameter monolithic penetrator. However, most segmented penetrators are launch pre-extended using either carrier rods or carrier tubes. Therefore a more natural selection of length would be the overall penetrator length.

Figure 7 shows the result predicted in the simulations for the segmented penetrator without carrier rods and the equivalent mass monolithic penetrators in terms of P/L where L is the length of the equivalent mass and diameter monolithic penetrator. The equivalent mass and length penetrator has the lowest penetrator efficiency, yet it out performed the others in terms of total penetration. The segmented penetrator is shown to be the most efficient. In Figure 8 the overall or launch length was used to determine P/L. Here the efficiency of the monolithic penetrators remains the same but the segmented penetrator is the least efficient.

Figure 9 shows P/L as a function of S/D. It can be shown, depending on the choice of length that penetration efficiency either increases or decreases with increasing S/D ratio. If length is taken to be that of a equivalent mass and diameter monolithic penetrator P/L increases with increasing S/D ratio. However, if overall length is chosen then P/L decreases with increasing S/D ratio.

4. CONCLUSIONS

4.1 The contribution to penetration of the carrier/spacer rods is significant. The results show closer agreement to the equivalent length monolithic penetrator than to that of a true segmented penetrator. The carrier rods have the effect of making the segmented penetrator behave more like a continuous rod than a segmented one.

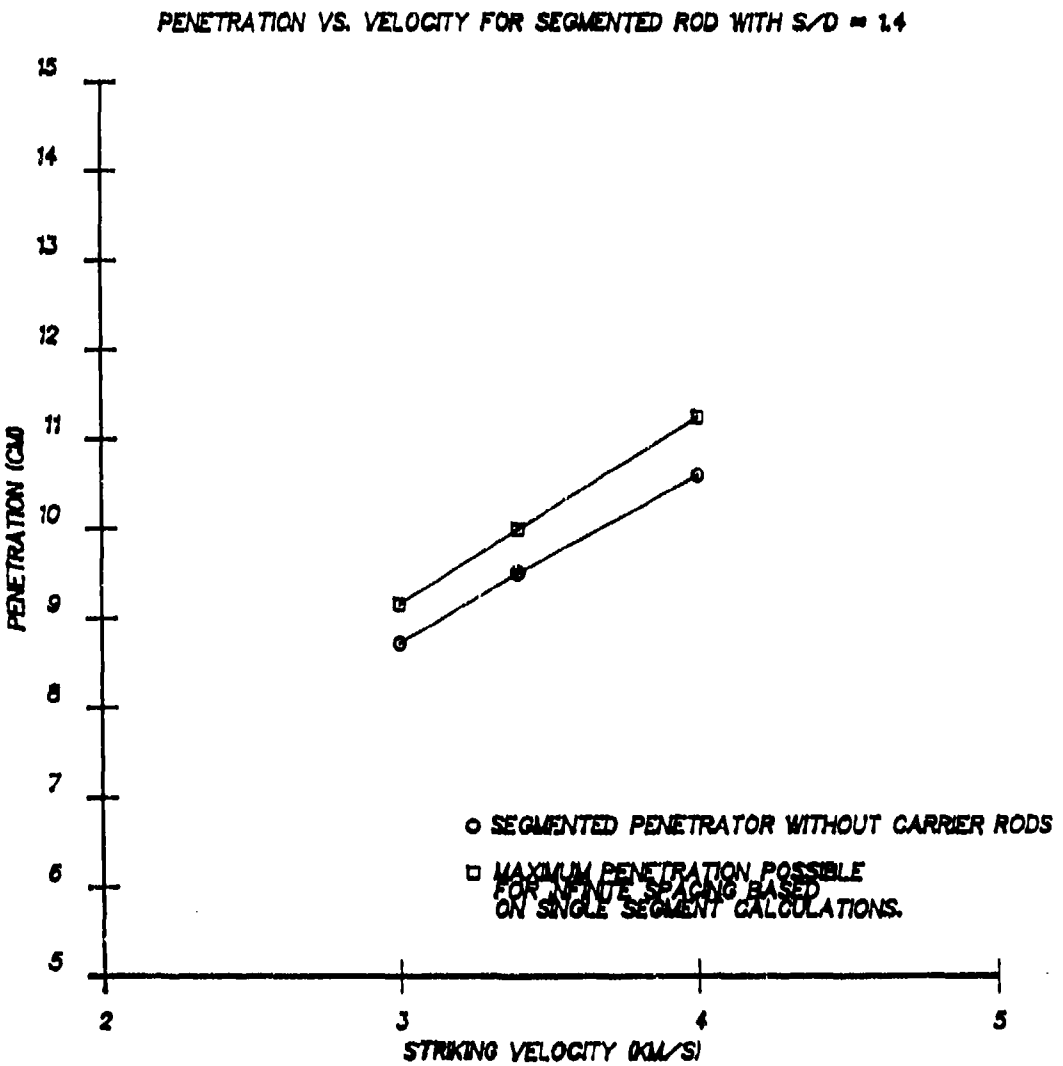

Figure 6. Predicted Penetration as a Function of Velocity.

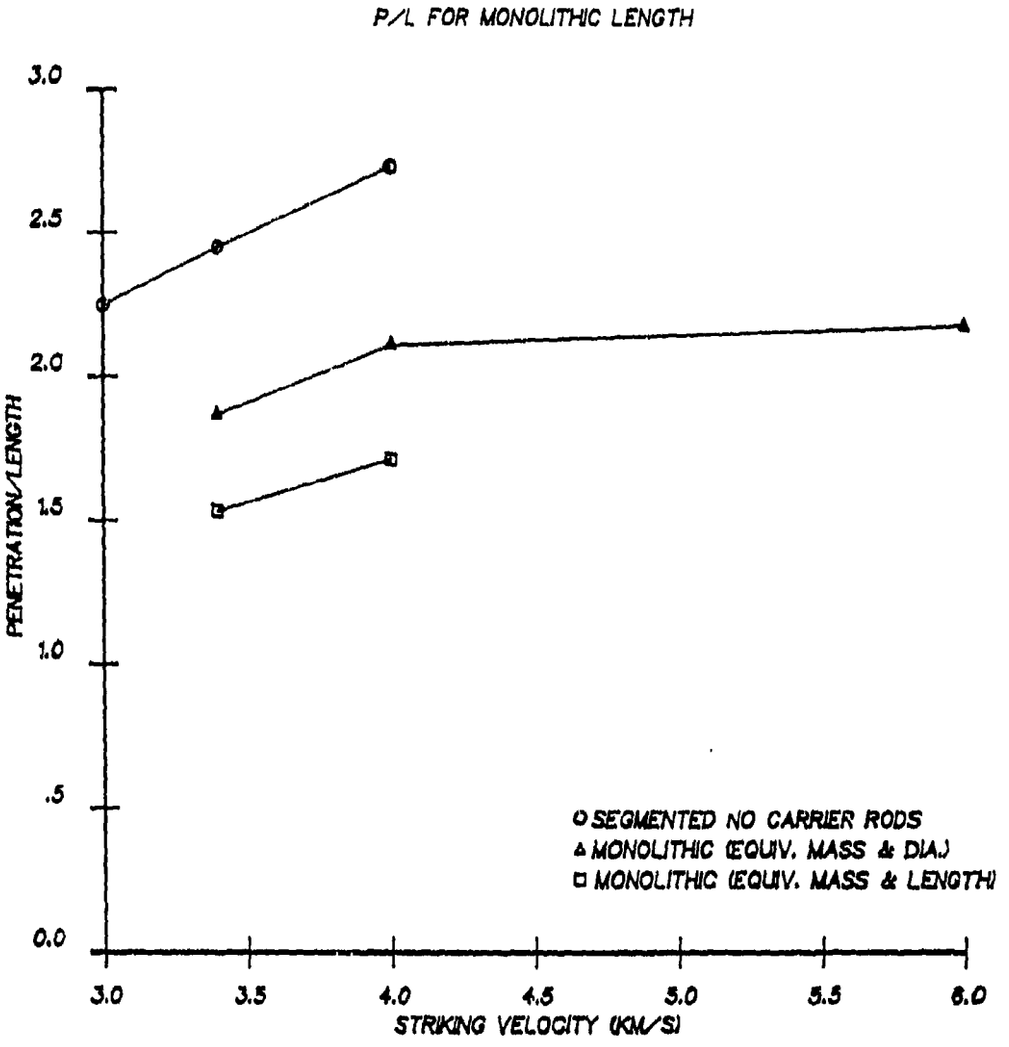

Figure 7. Penetration Efficiency Based on Monolithic Length.

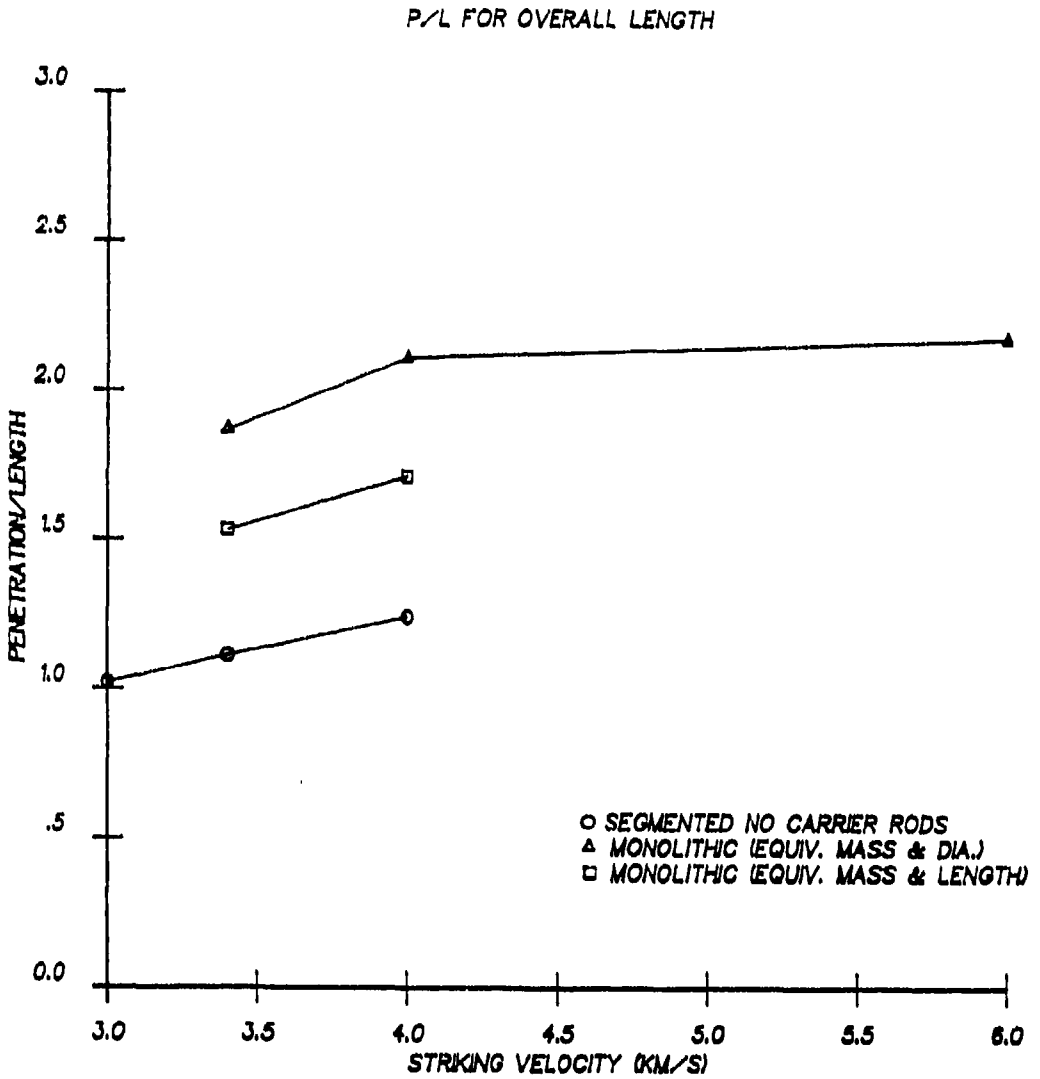

Figure 8. Penetration Efficiency Based on Overall Length.

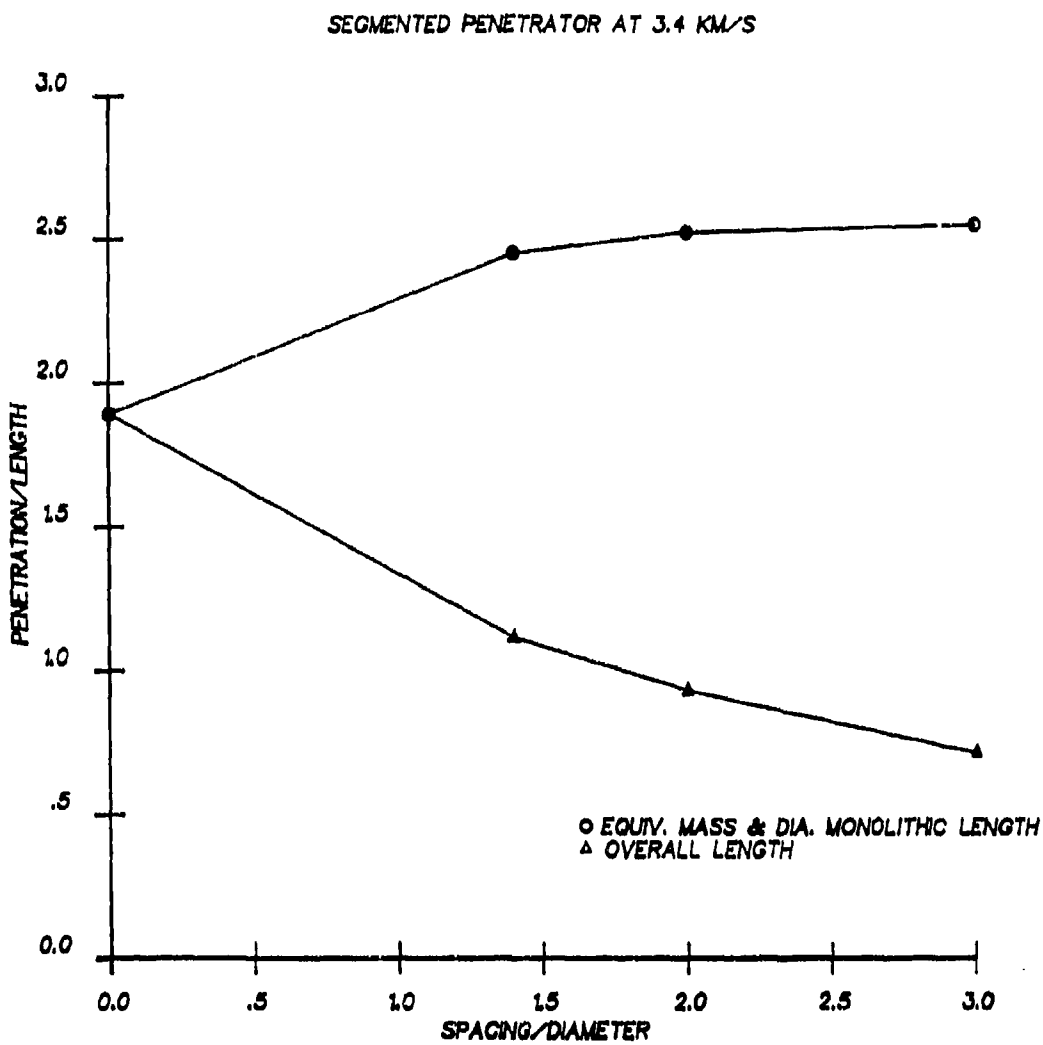

Figure 9. Penetration Efficiency as a Function of Segment Spacing. (Two Interpretations)

4.3 Of the penetrator configurations studied, the equivalent mass and length penetrator outperformed all others when measured in terms of penetration. This suggests that in many cases a monolithic penetrator can be more effective than a segmented one. The segmented penetrator has greater penetration than equivalent mass and diameter monolithic penetrators.

4.3 Increasing the spacing-to-diameter ratio increases the performance of segmented rods measured in terms of penetration. The optimum spacing for the segmented penetrator studied is between 2 and 3 diameters at a striking velocity of 2.4 km/s. Results suggest that increased spacing is needed at higher velocities to maintain optimum performance.

4.4 The use of penetration efficiency, the ratio of penetration to penetrator length (P/L), is not a good indicator of penetrator performance for segmented penetrators. Depending on the interpretation of length, monolithic or overall, conflicting conclusions can be drawn.

Next page is blank.

REFERENCES

1. Charters, A. C., "The Penetration of Rolled Homogenous Armor by Continuous and Segmented Rods at High Velocity: Theory and Experiments", General Research Corporation Technical Report CR-86-1031, April 1986.

2. Kucher, V., "Multiple Impacts on Monolithic Steel", Ballistic Research Laboratory Technical Report ARBRL-TR-02406, April 1982.

3. de Rosset, W. S. and Kimsey, K. D., "Calculation of Multiple Copper Rod Impacts on Steel Targets", Proc. Ninth International Symposium on Ballistics, Shrivenham, U. K., April 29-30, May 1, 1986.

4. Sedgwick, R. T., Waddell, J. L., and Wilkinson, G. M., "High Velocity Long Rod Impact: Theory and Experiment", Proc. Tenth International Symposium on Ballistics, San Diego, October 1987.

5. Charters, A. C., "The Penetration of Rolled Homogenous Armor by Continuous and Segmented Rods at High Velocity: Theory and Experiments", General Research Corporation Technical Report CR-87-1008, December 1986.

6. Bell, L. P., "Evaluation of Segmented and Solid Projectiles During Hypervelocity Flight and Impact", Arnold Engineering Development Center Technical Report AEDC-TRS-87-V6, March 1987.

7. Charters, A. C., and Menna, T. L., "Armor/Anti-armor Program: Advanced Penetrator Concepts Evaluation Program", General Research Corporation briefing package presented at the Armor/Anti-Armor Executive Steering Committee, Arlington, Virginia, August 25, 1987.

8. Charters, A. C., and Menna, T. L., "Armor/Anti-armor Program: Second Quarterly Review", General Research Corporation briefing package presented at the Impact Physics Team Second Quarterly Review, Lawrence Livermore National Laboratories, October 14-15, 1987.

9. Vrable, D. L., Rosenwasser, S. N., and Cheverton, "A Laboratory Railgun for Terminal Ballistics and Arc Armature Research Studies", Ballistic Research Laboratory Contractor Report BRL-CR-572, June 1987.

10. Matuska, D. A. and Osborn, J. J.,"HULL Technical Manual," vol I, Orlando Technology Incorporated, 1986.

11. Matuska, D. A. and Osborn, J. J.,"HULL Users Manual," vol II, Orlando Technology Incorporated, 1986.

12. Hancock, J. W., and Mackenzie, A. C., J. Mech. Phys. Solids, 24, 147.

13. Silsby, G. F., Ballistic Research Laboratory, telephone conversation with A. Charters of General Research Corporation, October 1, 1988.

14. Silsby, G. F., private communication, October 17, 1988.

15. Charters, A. C., letter to Bruce Burns of Ballistic Research Laboratory, dated October 25, 1988.

16. Wilkins, M. L., in B. Adler et al. (Eds.),"Methods in Computational Physics," Academic Press, New York, 1964.

17. Nicholas, T., "Dynamic Tensile Testing of Structural Materials Using a Split Hopkinson Bar Apparatus", Air Force Wright Aeronautical Laboratories Technical Report AFWAL-TR-80-4053, October 1980.

18. Johnson, G. R. and Cook, W. H., "A Contitutive Model and Data for Metals Subjected to Large Strains, High Strain Rates and High Temperatures", Proc. Seventh International Symposium on Ballistics, The Hague, Netherlands, April 19-21, 1983.

APPENDIX A

MATERIAL PROPERTIES AND EQUATION OF STATE DATA

APPENDIX

Material Properties and Equation of State Data

	4340 FI	TUNGSTEN
Ambient density (g/cc)	7.86	17.3
Ambient sound speed (cm/s)	4.61e5	4.0e5
Shock velocity, particle velocity slope	1.73	1.268
Initial Grunesen ratio	1.69	1.43
Minimum Pressure (dynes/cm**2)	-35.e9	-10.e9
Poisson's ratio	0.26	0.3
Atomic weight	55.85	184.
DeBye's temperature (K)	355	270
Vapor coefficient	0.25	0.2
Ambient energy per unit mass (ergs/g)	0.0	0.0
Ambient melt energy per unit mass (ergs/g)	7.4e9	4.77e9
Fusion energy per unit mass (ergs/g)	2.74e9	1.84e9
Sublimation energy per unit mass (ergs/g)	74.2e9	46.e9
Ambient vaporisation energy per unit mass (ergs/g)	22.4e9	13.6e9
Ambient energy per unit mass at end of vaporisation (ergs/g)	86.8e9	58.4e9
Initial yield strength (dynes/cm**2)	11.4e9	14.e9
Saturation yield strength (dynes/cm**2)	11.4e9	19.3e9
Plastic strain at saturation yield strength	0.01	0.3
Yield strength ratio for first point on thermal softening curve	1.0	1.0
Energy ratio for first point on thermal softening curve	0.5	0.5
Yield strength ratio for second point on thermal softening curve	1.0	1.0
Energy ratio for second point on thermal softening curve	1.0	1.0
Second coefficient in Hugoniot pressure curve	0.0	0.0
Third coefficient in Hugoniot pressure curve	0.0	0.0
Ultimate failure stress	1.e50	1.e50
Ultimate failure strain	0.16	0.16

BRL MANDATORY DISTRIBUTION LIST

No of Copies	Organization
(Unclass., unlimited) 12	Administrator
(Unclass., limited) 2	Defense Technical Info Center
(Classified) 2	ATTN: DTIC-DDA
	Cameron Station
	Alexandria, VA 22304-6145
1	HQDA (SARD-TR)
	Washington, DC 20310-0001
1	Commander
	US Army Materiel Command
	ATTN: AMCDRA-ST
	5001 Eisenhower Avenue
	Alexandria, VA 22333-0001
1	Commander
	US Army Laboratory Command
	ATTN: AMSLC-DL
	Adelphi, MD 20783-1145
2	Commander
	Armament RD&E Center
	US Army AMCCOM
	ATTN: SMCAR-MSI
	Picatinny Arsenal, NJ 07806-5000
2	Commander
	Armament RD&E Center
	US Army AMCCOM
	ATTN: SMCAR-TDC
	Picatinny Arsenal, NJ 07806-5000
1	Director
	Benet Weapons Laboratory
	Armament RD&E Center
	US Army AMCCOM
	ATTN: SMCAR-LCB-TL
	Watervliet, NY 12189-4050
1	Commander
	US Army Armament, Munitions and Chemical Command
	ATTN: SMCAR-ESP-L
	Rock Island, IL 61299-5000
1	Commander
	US Army Aviation Systems Command
	ATTN: AMSAV-DACL
	4300 Goodfellow Blvd.
	St. Louis, MO 63120-1798
1	Director
	US Army Aviation Research and Technology Activity
	Ames Research Center
	Moffett Field, CA 94035-1099

No of Copies	Organization
1	Commander
	US Army Missile Command
	ATTN: AMSMI-RD-CS-R (DOC)
	Redstone Arsenal, AL 35898-5010
1	Commander
	US Army Tank Automotive Command
	ATTN: AMSTA-TSL (Technical Library)
	Warren, MI 48397-5000
1	Director
	US Army TRADOC Analysis Command
	ATTN: ATAA-SL
	White Sands Missile Range, NM 88002-5502
(Class. only) 1	Commandant
	US Army Infantry School
	ATTN: ATSH-CD (Security Mgr.)
	Fort Benning, GA 31905-5660
(Unclass. only) 1	Commandant
	US Army Infantry School
	ATTN: ATSH-CD-CSO-OR
	Fort Benning, GA 31905-5660
1	AFWL/SUL
	Kirtland AFB, NM 87117-5800
(Class. only) 1	The Rand Corporation
	P.O. Box 2138
	Santa Monica, CA 90401-2138
1	Air Force Armament Laboratory
	ATTN: AFATL/DLODL
	Eglin AFB, FL 32542-5000

Aberdeen Proving Ground

Dir, USAMSAA
ATTN: AMXSY-D
AMXSY-MP, H. Cohen

Cdr, USATECOM
ATTN: AMSTE-TO-F

Cdr, CRDEC, AMCCOM
ATTN: SMCCR-RSP-A
SMCCR-MU
SMCCR-MSI

AUTHOR'S DISTRIBUTION LIST

No. of Copies — Organization

2 Orlando Technology Inc.
ATTN: Mr. D. Maduska
Mr. J. Osborne
P.O. Box 855
60 Second Street
Shalimar, FL 32579

1 General Research Corporation
ATTN: Dr. A. Charters
P.O. Box 6770
5383 Hollister Avenue
Santa Barbara, CA 93160-6770

3 Sandia National Laboratory
ATTN: M. Kipp
P. Yarrington
W. Herrmann (Org. 150)
Albuquerque, NM 87115

1 General Dynamics
ATTN: J. H. Cuadros
P.O. Box 2507
Pomona, CA 91745

2 Honeywell Inc.
ATTN: Dr. G. Johnson
R. Stryk
7225 Northland Drive
Brooklyn Park, MN 55428

1 Systems, Science and Software
ATTN: Dr. R. Sedgwick
La Jolla, CA 92038

1 Orlando Technology Inc.
ATTN: Mr. N. Piburn
2340 Alamo SE, Suite 101
Albuquerque, NM 87106

4 Commander
Naval Surface Warfare Center
ATTN: Paula Walter
Kenneth Kiddy
F. J. Zerilla
Lisa Meusi
10901 New Hampshire Ave.
Silver Spring, MD 20903-5000

2 AFATL/DLJW
ATTN: Dr. W. Cook
M. Nixon
Eglin AFB, FL 32542

4 Los Alamos National Laboratory
ATTN: Dr. E. Cort
Dr. R. Fujita
Dr. R Karpp (MS P940)
Dr. M. Burkett
P.O Box 1663
Los Alamos, NM 87545

USER EVALUATION SHEET/CHANGE OF ADDRESS

This laboratory undertakes a continuing effort to improve the quality of the reports it publishes. Your comments/answers below will aid us in our efforts.

1. Does this report satisfy a need? (Comment on purpose, related project, or other area of interest for which the report will be used.) _____

2. How, specifically, is the report being used? (Information source, design data, procedure, source of ideas, etc.) _____

3. Has the information in this report led to any quantitative savings as far as man-hours or dollars saved, operating costs avoided, or efficiencies achieved, etc? If so, please elaborate. _____

4. General Comments. What do you think should be changed to improve future reports? (Indicate changes to organization, technical content, format, etc.) _____

BRL Report Number _____ Division Symbol _____

Check here if desire to be removed from distribution list. ____

Check here for address change. ____

Current address: Organization _____
Address _____

----------FOLD AND TAPE CLOSED----------

Director
U.S. Army Ballistic Research Laboratory
ATTN: SLCBR-DD-T(NEI)
Aberdeen Proving Ground, MD 21005-5066

OFFICIAL BUSINESS
PENALTY FOR PRIVATE USE $300

BUSINESS REPLY LABEL
FIRST CLASS PERMIT NO. 12062 WASHINGTON D.C

POSTAGE WILL BE PAID BY DEPARTMENT OF THE ARMY

NO POSTAGE NECESSARY IF MAILED IN THE UNITED STATES

[redacted]

Director
U.S. Army Ballistic Research Laboratory
ATTN: SLCBR-DD-T(NEI)
Aberdeen Proving Ground, MD 21005-9989